Journal of Advanced Ceramics
2012, 1(1): 2-23
DOI: 10.1007/s40145-012-0002-4 ISSN 2226-4108

Review

Electrospinning of ceramic nanofibers: Fabrication, assembly and applications

Hui WU, Wei PAN*, Dandan LIN, Heping LI

State Key Lab of New Ceramic and Fine Processing, Department of Materials Science and Engineering, Tsinghua University, Beijing 100084, China

Received March 1, 2012; Accepted March 5, 2012

Abstract: This paper provides a brief review of current research activities that focus on the synthesis and controlled assembly of inorganic nanofibers by electrospinning, their electrical, optical and magnetic properties, as well as their applications in various areas including sensors, catalysts, batteries, filters and separators. We begin with a brief introduction to electrospinning technology and a brief method to produce ceramic nanofibers from electrospinning. We then discuss approaches to the controlled assembly and patterning of electrospun ceramic nanofibers. We continue with a highlight of some recent applications enabled by electrospun ceramic nanofibers, with a focus on the physical properties of functional ceramic nanofibers as well as their applications in energy and environmental technologies. In the end, we conclude this review with some perspectives on the future directions and implications for this new class of functional nanomaterials. It is expected that this review paper can help the readers quickly become acquainted with the basic principles and particularly the experimental procedure for preparing and assembly of 1D ceramic nanofiber and its arrays.

Key words: electrospinning; nanofibers; functional ceramics; catalyst

1 Introduction

One-dimensional (1D) nanostructures such as nanowires, nanotubes, nanoribbons and nanofibers are continuing to be at the forefront of nanoscience and nanotechnology [1-8]. In particular, ceramic with 1D nano-architectures received increasing interest since it provides a good material system to investigate the dependence of electrical, optical, thermal and mechanical properties on dimensionality and size reduction [9-14]. 1D ceramic nanomaterials with their large surface-to-volume ratio have the potential for use in various applications where high porosity is desirable [11-13]. For example, inorganic nanowires are expected to play an important role as promising building blocks for nanoscale electronic [9,10,15], optoelectronic [15,16] and sensor device [12,17,18]. Most recently, ceramic nanowires have been explored as effective electrode materials for electrochemical energy storage devices [19,20]. In the past two decades, worldwide efforts in both the theory and the experimental investigation of growth, characterization and applications of 1D inorganic nanostructures have resulted in a mature, multidisciplinary field. For practical application of 1D ceramic nanomaterials,

* Corresponding author.
E-mail: panw@tsinghua.edu.cn

scalable materials production and convenient devices integration are extremely important. Technological advances over have resulted in the realization of several competing processes for fabricating nanometer-size ceramic materials. So far, many kinds of 1D ceramic nanomaterials have been successfully synthesized by a rich variety of methods, and the detailed research information on these 1D nanostructures can be readily seen in the pertinent literature [10,15,18,21-23].

Among various chemical or physical synthetic approaches, electrospinning appears to be the most straightforward and versatile technique for generating 1D nanostructures [24-26]. Electrospinning was first patented in the US in 1902; however, the process was largely forgotten until the 1990s [27,28]. Electrospinning is currently the only technique that allows the fabrication of continuous fibers with diameters down to a few nanometers. Fibers with complex architectures, such as core–shell fibers or hollow fibers, can be produced by special electrospinning methods [24-26]. It is also possible to produce structures ranging from single fibers to ordered arrangements of fibers. Electrospinning is not only employed in university laboratories, but is also increasingly being applied in industry. The scope of applications, in fields as diverse as optoelectronics, sensor technology, catalysis, filtration, and medicine, is very broad [27,29,30]. However, electrospinning has been largely limited to the fabrication of nanofibers of organic polymers materials, including synthetic and natural polymers, polymer alloys, and polymers loaded with chromophores, nanoparticles, or active agents, as it is relatively convenient to prepare a polymer solution or melt with appropriate rheological properties required for electrospinning [27,29,30]. Metals and ceramics are usually considered to be not directly spinnable [27,31] . Recent efforts by several research groups have made it possible to generate ceramic nanofibers using electrospinning technique [24,28-30, 32-35]. This review will present a brief overview of recent progress in this research area, with a focus on the work carried out in our group [16,35-58]. After briefly introducing the basic principles of electrospinning, this paper will review the general experimental procedures for the preparation of electrospinning ceramic nanofibers, and will highlight several unique features associated with the technique and illustrate the potential of electrospinning in future research related to ceramic processing. We will also discuss the controlled assembly and patterning of electrospun ceramic nanofibers. Finally, we will highlight some recent achievements on the study of physical properties of electrospun ceramic nanofibers and their practical applications in the context of nanoelectronics, catalysis, environmental science, and energy technology [16,35-56]. By the end, we also provide some personal perspectives on the future development of this technique. It is expected that this review paper can help the readers quickly become acquainted with the basic principles and particularly the experimental procedure for preparing and assembly of 1D ceramic nanofiber and its arrays.

2 Principle of electrospinning

Electrospinning is based on inducing static electrical charges on the molecules of a solution at such a density that the self-repulsion of the charges causes the liquid to stretch into a fiber in an electric field [27]. Provided there is no breakage in the stretched solution, a single strand of continuous fiber is formed upon solvent evaporation. When a high voltage is applied to the solution, the ohmic current distributes the charges throughout the molecules [27]. As the solution is ejected from the spinneret tip, the ohmic current transits to a predominantly convective current. The charges are transported from the electrospinning tip to the target through the deposition of the fiber. The current stops oscillating when the deposition becomes stable [29]. This can be used to monitor the spinning process. The electrical charges used for electrospinning can be positive, negative or both (alternating current). Although most reported electrospinning experiments were carried out using a positive potential, it has been shown that a negative potential produces nanofibers with a narrower diameter distribution [59,60]. This was explained by the fact that electrons can be dispersed more rapidly and uniformly than the much heavier protons.

In a typical electrospinning setup, a high-voltage source is connected to a metallic needle, which is attached to a solution reservoir (Fig. 1). The needle has a relatively small orifice that concentrates the electric charge density on a small pendant drop of solution. Although a metallic spinneret such as a needle is convenient for the application of charge to the solution, the process also works if a high voltage is applied to the solution using a dedicated electrode with a

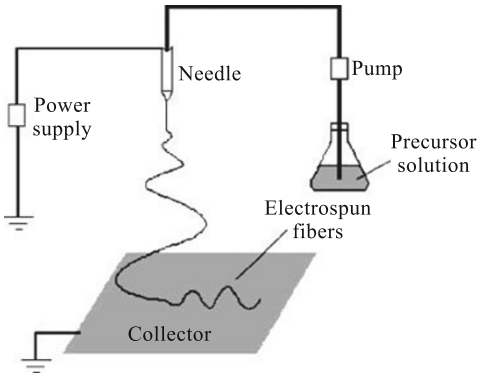

Fig. 1 Schematic drawing of the electrospinning apparatus. Reprinted with permission from Wu H, Pan W, J. Am. Ceram. Soc. 2006; 89: 699-701. Copyright 2005 The American Ceramic Society

nonconducting spinneret. A porous cylinder has also been used for electrospinning, and it is possible to induce charges on a free solution droplet without direct contact to form a fiber. The theoretical modeling of a viscous leaky dielectric solution subjected to a critical voltage showed that it becomes unstable in an electric field when the surface tension can no longer maintain its static equilibrium [27,31,59]. At this voltage, protrusions form on the solution surface and jets of solution are ejected. Any perturbation or nonuniformity on the solution surface will concentrate charges in regions with higher curvature. If the curvature is sufficiently large for the potential difference between such a region and the collector to reach a critical value, the solution erupts from the surface and accelerates towards the collector. This has given rise to numerous designs in which drums, spikes, ridges and disks have been used to dispense the solution for electrospinning. The diameter and morphology of electrospun nanofibers can be controlled by adjusting the following parameters during electrospinning [27,31,59]:

1. Molecular weight, molecular-weight distribution and architecture (branched, linear etc.) of the polymer;

2. Solution properties (viscosity, conductivity and surface tension);

3. Electric potential, flow rate and concentration;

4. Distance between the capillary and collection screen;

5. Ambient parameters (temperature, humidity and air velocity in the chamber);

6. Motion of target screen (collector);

7. Needle gauge.

3 Electrospinning of ceramic nanofibers

Electrospinning technique has been recognized as a fabrication method for polymer and carbon nanofibers [59]. Since 2002, electrospinning has been further explored as a high efficiency method for the generation of 1D ceramic nanofibers [26,29,32]. In the past decade, various ceramic nanofibers are fabricated by the combination of two conventional techniques: electrospinning and sol-gel [32,34]. Generally, ceramic nanofibers are made by the electrospinning of ceramic precursors in the presence of polymer followed by calcination at higher temperatures. In order to generate well-controlled and high-quality ceramic nanofibers by electrospinning, one typically process has to use the following procedure:

(1) Preparation of an electrospinning solution containing a polymer and sol-gel precursor to the ceramic material,

(2) Electrospinning of the solution under appropriate conditions, generate precursor nanofibers containing inorganic precursor and polymer assistant materials.

(3) Calcination of the precursor nanofibers at high temperature to remove polymers and obtain the ceramic phase.

Various oxide nanofibers can be synthesized by this approach. Notable examples includes ZnO, CuO, NiO, TiO_2, SiO_2, Co_3O_4, Al_2O_3, SnO_2, Fe_2O_3, $LiCoO_2$, $BaTiO_3$, $LaMnO_3$, $NiFe_2O_4$ and $LiFePO_4$ [16,26,27,29, 30,35,45,46,51-54,61-78]. A typical spinnable precursor solution should contain a salt precursor, a polymer and a relatively volatile solvent such as ethanol, water, isopropanol, chloroform, and dimethylformamide (DMF) [26,59-76]. Poly(vinyl alcohol) (PVA) is one of the most popular polymers employed as a matrix due to its high solubility in water and its good compatibility with many salts, including zinc acetate and copper nitrate [49]. In addition, other polymers, such as poly(vinyl pyrolidone) (PVP), poly(vinyl acetate) (PVAc), poly-acrylonitrile (PAN), poly(methyl methacrylate) (PMMA), and poly(acrylic acid) (PAA) have also been widely used [26,27,31,35,69].

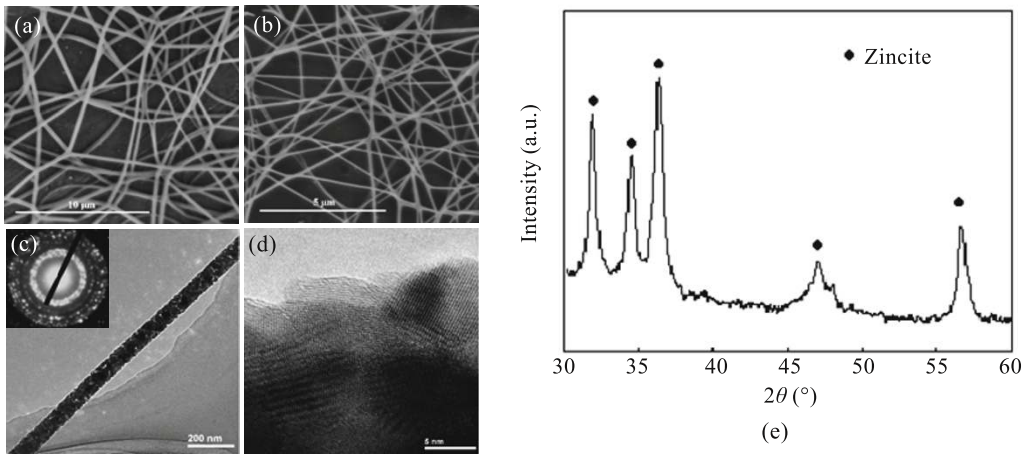

Fig. 2 (a) Field emission scanning electron microscopy image of the precursor fibers collected in random orientation. The fibers have an average diameter of about 230 nm. (b) ZnO nanofibers prepared by calcination of the precursor fibers at 500 ℃ for 4 h. The fibers remain continuous, with a uniform morphology. The diameter of the ZnO nanofibers decreased to 70 nm. (c) Transmission electron microscopy (TEM) image of a single ZnO nanofiber. Inset: the selected area electron diffraction pattern. (d) High-resolution TEM (HRTEM) image of the same sample, indicating the polycrystalline structure of the calcined fiber. (e) X-ray diffraction results for zinc acetate/polyvinyl alcohol precursor fibers' calcination at 500 ℃ for 6h [43]. Reprinted with permission from Lin D D, Pan W, Wu H, J. Am. Ceram. Soc. 2007; 90: 71-76. Copyright 2006 The American Ceramic Society

One advantage of electrospinning method for ceramic nanofiber processing is the component of nanofibers can be easily controlled by tuning electrospinning precursor solutions, and the fiber morphologies can be adjusted during electrospinning and calcination processes. For example, ultra-thin fibers of zinc oxide can be prepared by sol–gel processing and the electrospinning technique using PVA and zinc acetate as precursors [36,40,43,47-49,70, 72]. After electrospinning and calcination of the precursor fibers, ceramic ZnO nanofibers were fabricated as demonstrated by X-ray diffraction (XRD) [36,43]. TEM images of the nanofibers after calcinations indicated that the fibers had a smooth surface, and were formed through the agglomeration of ZnO nanoparticles with domain sizes of about 10 nm [36,43]. Experimental results show that the diameter of the precursor fibers can be controlled by adjusting the concentration of zinc acetate, and the morphology of the inorganic ZnO fibers is influenced by calcination time [36,43]. One advantage of electrospinning method for ceramic nanofiber processing is the component of nanofibers can be easily controlled by tuning electrospinning precursor solutions, and the fiber morphologies can be adjusted during electrospinning processes [16,39].

Doping or incorporation of foreign materials into a solid ceramic matrix material is often required for many applications such as catalysis and chemical sensors [12]. One remarkable feature that distinguishes the electrospinning approach from other techniques for preparing ceramic nanofibers is that it is very simple and convenient to incorporate or encapsulate other materials into the nanofibers and nanotubes. In an

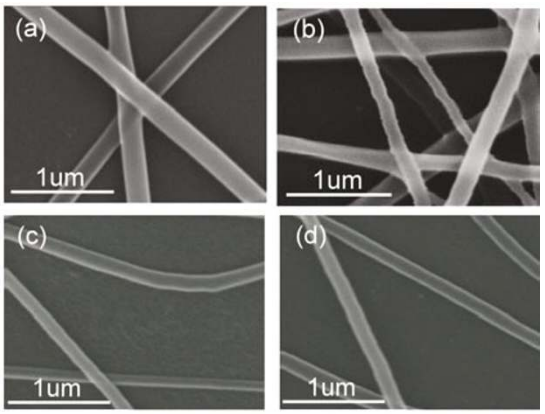

Fig. 3 Scanning electron microscopy images of polyvinyl alcohol (PVA)/zinc acetate composite fibers electrospun at the voltage of 20 kV, with various Al contents (PVA wt%510%): Al at.%5(a) 0%, (b) 1.0%, (c) 2.0%, (d) 3.0% in aluminum-doped zinc oxide nanowires [39]. Reprinted with permission from Wu H, Lin D D, Zhang R, Pan W, J. Am. Ceram. Soc. 2008; 91: 656-659. Copyright 2007 The American Ceramic Society

electrospinning process, functional materials (molecules or nanoparticles) can be easily doped or incorporated into nanofibers by adding these materials or their precursors to the spinning solutions. For example, Lin *et al.* fabricated aluminum-doped zinc oxide (AZO) nanofibers with precisely controlled Al dopant concentration by adding aluminum nitrate in electrospinning solutions (Fig. 3) [16,39]. The diameter of AZO nanofibers decreased and became uniform when the concentration of Al increased from 0 to 3.0 at.%. The dependence of the morphology and diameter of the electrospun nanofibers on the processing parameters, including PVA concentration, applied voltage, and the Al dopant, was investigated in their research. It was found that the viscosity and conductivity were of most importance to the morphology of the e-spinning fibers, given constant electric field strength and flow rate [16,39]. Another example for this controlled doping is Ag-ZnO nanofibers by electrospinning [47,48]. Ag nanoparticles with controlled concentration have been successfully loaded in ZnO nanofibers by Lin *et al.* (Fig. 4).

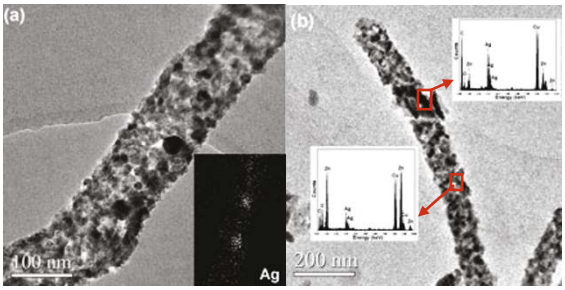

Fig. 4 TEM images of the Ag-ZnO composite nanowires: (a) 10.0 at. % Ag. inset: EDX mapping of Ag element along the nanowire; (b) 15.0 at. % Ag. Insets: typical EDX microanalysis on selected areas of a single nanowire [47]. Reprinted with permission from Lin D D, Wu H, Zhang R, Pan W, Chem. Mater. 2009; 21: 3479-3484. Copyright 2009 American Chemical Society

Electrospinning technique can also be used for fabricating nanofibers composed by non-oxide ceramics including carbide, boride, nitride, silicide and sulphide [38,50,79-87]. Wu *et al.* synthesized nitride nanofibers via electrospinning for the first time [50]. Group III N alloys, particularly GaN, have a huge potential for revolutionary semiconductor device configurations. Extremely long GaN nanofibers on a large scale can be synthesized based on electrospinning. The strategy to obtain GaN nanofibers can be divided into three steps: (1) The electrospinning of precursor composite nanofibers that comprise polymer and gallium nitrate; (2) Calcination of the composite nanofibers in air to thoroughly remove organic components and to form gallium oxide nanofibers; (3) In situ conversion of the as-prepared oxide nanofibers into nitride nanofibers in an ammonia atmosphere at high temperature [50]. SEM image shows that the continuous structure of the initial Ga_2O_3 nanofiber was maintained after ammonization. The length of the synthesized GaN nanofibers could reach the centimeter scale, and the average fiber diameter is only 40 nm, which indicates an ultrahigh aspect ratio of the GaN nanofibers (Fig. 5a). TEM images (Fig. 5b) also reveal the fibrillar structure of the ammoniated samples. A selected-area electron-diffraction (SAED) pattern shows that the nanofibers are polycrystalline, and a

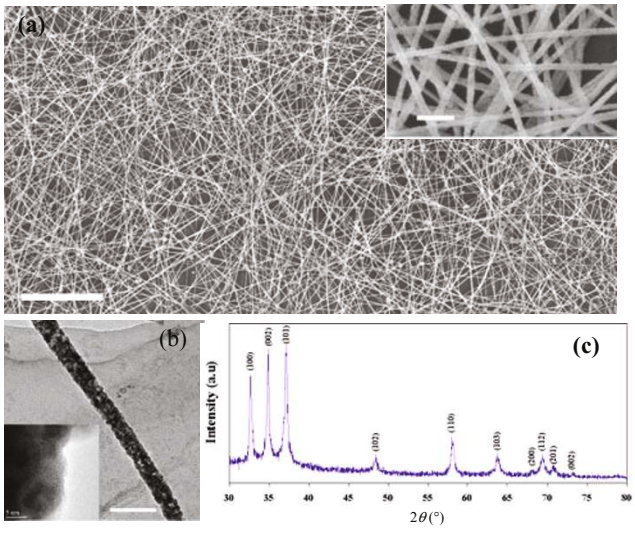

Fig. 5 (a) SEM image of synthesized GaN nanofibers. Scale bar: 5 μm. Inset: SEM image with higher magnification. Scale bar: 200 nm. (b) TEM image of a single GaN nanofiber. Scale bar: 100 nm. Upper inset depicts a corresponding EDX pattern, lower left inset is a high-resolution TEM image. Scale bar: 5 nm. (c) XDR pattern of synthesized nanofibers [50]. Reprinted with permission from Wu H, Lin D D, Zhang R, Zhang C. Pan W, Adv. Mater. 2009; 21: 227-231. Copyright 2009 WILEY-VCH Verlag GmbH & Co. KGaA, Weinheim

high resolution TEM image indicates that the crystalline size of the nanofiber is less than 10 nm (insets of Fig. 5b). This approach will be applicable to the synthesis of other nitride nanofibers such as InN, AlN, and InGaN. It is expected that this technique will make the large-scale production and assembly of nitride functional nanomaterials with practical applications possible [50].

Lin *et al.* demonstrated that using the electrospinning technique coupled with a thermal treatment approach, ZnS nanofibers can be prepared by sulfurizing the electrospun ZnO nanofibers (as a template) at 500 ℃ in an H2S atmosphere (Fig. 6) [38]. The ZnS nanofibers were found to be polycrystalline, with an average grain size of 20 nm (Fig. 6d). The morphology of ZnS nanofibers was found to be rough and uneven, which was considered to be correlated with the processing conditions. Their study demonstrated that electrospinning could be a general approach of fabricating 1D-nanostructured sulfide with rough surface and high surface area for potential applications in nanoscale devices like high performance sensors [38].

4 Controlled assembly of ceramic nanofibers

Well-aligned and highly ordered structures are often required for device applications, especially in the fabrication of electric and photonic devices like field effect transistors, sensors and diodes. Many approaches have been developed to control the alignment of electrospun nanofibers. Xia group developed a gap technique, as shown in Fig. 7a, by which one can collect the electrospun nanofibers as a uniaxially aligned arrays over a large area [24,27,29,30,32-34,88]. The setup is essentially the same as the conventional one except for the introduction of an insulating (e.g. made of air, quartz, or polystyrene) gap in the middle of the collector, with a width that can be varied from hundreds of micrometers to several centimeters. The insulating gap makes the electric field lines in the vicinity of the collector split into two fractions pointing toward opposite edges of the gap (see the electrostatic force analysis in Fig. 7b). The as-spun, charged nanofibers are expected to experience electrostatic forces from two sources: the strong external field (F1) between the spinneret and the collector, and the repulsion between adjacent, charged fibers (F2). As a result, the fibers are stretched perpendicular to the edges of the gap [33]. Since the fibers can keep highly charged after deposition, the strong repulsion between the deposited and incoming nanofibers can facilitate a parallel alignment between them as this alignment has the lowest energy. Therefore, the alignment can be significantly improved as the deposition is increased. By using this modified electrospinning technique, well-aligned ceramic nanofiber arrays (Fig. 7) or single nanofiber deposited in controlled directions can be fabricated.

Our group developed a newly modified electrospinning technique for generating highly oriented ceramic nanofibers with a length of several centimeters. Very different from the conventional electrospinning process, the fibers are collected between the electrodes [41]. The experimental configuration for our modified electrospinning setup is illustrated in Fig. 8a. Unlike the conventional setup, a metallic triangular tip without any solution supply system was used as the electrospinning source. The tip

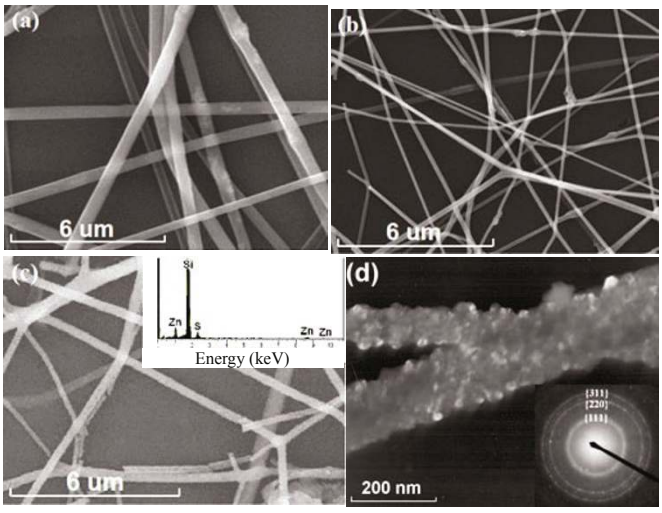

Fig. 6 SEM image of as-spun PVP–zinc acetate composite nanofibers (a), after annealing at 500 ℃ in air for 1 h (b), after subsequent annealing at 500 ℃ in a H_2S atmosphere for 2 h (c), and a dark-field transmission electron microscopy image there of (d). An energy-dispersive X-ray spectroscopy result and electron-diffraction pattern recorded from the ZnS nanofibers are inserted, respectively [38]. Reprinted with permission from Lin D D, Wu H, Zhang R, Pan W, J. Am. Ceram. Soc. 2007; 90: 3664-3666. Copyright 2007 The American Ceramic Society

was prepared by cutting down a 1-mm-thick aluminum sheet into a 1- 5 cm rectangle with a triangular tip. The apex angle of the triangular was set as 60°. The tip was used as the electrospinning source; it helped to establish a Tylor cone while electrospinning. A grounded coin was placed close to the aluminum sheet as the counter electrode of the system. A bundle of aligned electrospun fibers was then formed between the spinning tip and the collector (Fig. 1c). The fibers were then transferred on a silicon wafer. The key to success is the reduction of interelectrode distance and the use of an ultra strong electric field, which is about six times higher than conventional conditions [41].

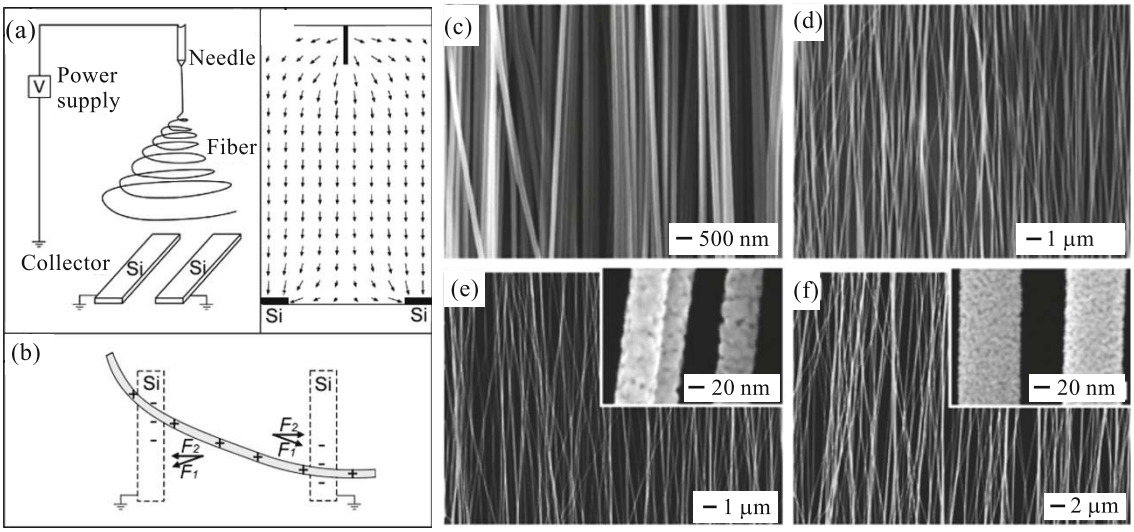

Fig. 7 (a) Schematic illustration of the setup for collecting nanofibers as a uniaxially aligned array. The collector contains an insulating void, such as the air gap between two strips of silicon wafers. (b) Electrostatic force analysis of a charged nanofiber spanning across two silicon strips. The orientation of the nanofiber is mainly controlled by the stretching force originating from the attractive electrostatic forces. (c)-(f) SEM images of uniaxially aligned nanofibers made of (c) carbon, (d) anatase TiO_2, (e) $NiFe_2O_4$, (f) TiO_2/PVP [29]. Reprinted with permission from Li D, Wang YL, Xia YN. Nano Lett 2003; 3: 1167-1171. Copyright 2003 American Chemical Society

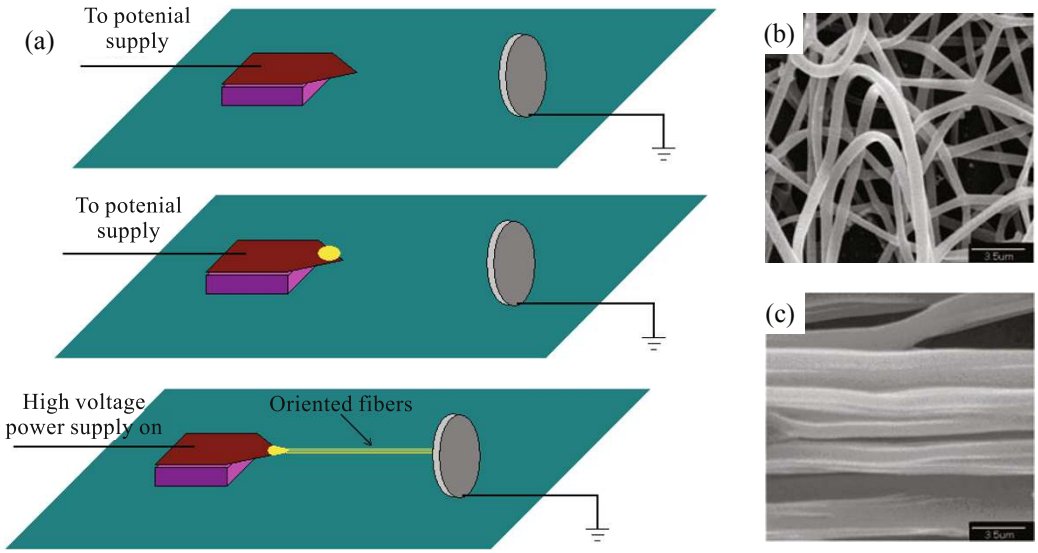

Fig. 8 (a) Schematic illustration of the modified electrospinning process for preparing aligned fibers. (b) SEM image of randomly arranged polyvinyl acetate (PVA)/zinc acetate composite fibers prepared by the conventional electrospinning method; (c)SEM images of random nanofibers and oriented fibers obtained by the modified electrospinning method [41]. Reprinted with permission from Wu H, Lin D D, Zhang R, Pan W. J Am Ceram Soc 2007; 90: 632-634. Copyright 2006 The American Ceramic Society

5 Properties and applications

5.1 Electrical transfer properties and FET devices

Our group reported the assembly and electrical properties of ultralong copper oxide (CuO) nanofibers prepared by electrospinning method [35]. The prepared CuO nanofibers were polycrystalline, with diameter of 60 nm and length over 100 μm. By using a designed fiber collector, the electrospun CuO nanofiber was deposited bridging two paralleled electrodes. Electrical measurement was conducted between the two electrodes. The conductivity of individual CuO nanofiber was measured to be 3×10^{-3} S/cm. Field effect transistor behavior in single CuO nanofiber was also observed, showing that CuO nanofiber was intrinsic p-type semiconductor [35]. Another research in our group performed electrical measurement on single ZnO nanofibers. FET behavior in single ZnO nanofiber was also observed, showing that the ZnO nanofiber was an intrinsic n-type semiconductor [43].

Highly oriented GaN nanofibers were fabricated by electrospinning. This technique indicated the possibility of precisely locating a patterned GaN nanofiber with designed orientation, which is favorable for some practical applications such as electrical devices and lasers [50]. As an example, we assembled a single electrospun GaN nanofiber into a field-effect transistor device, which is schematically shown in the inset of Fig. 9d. The current–voltage (I_{sd}–V_{sd}) characteristics of a GaN nanofiber FET device at different gate voltages (from +60V to –60V with a 30V

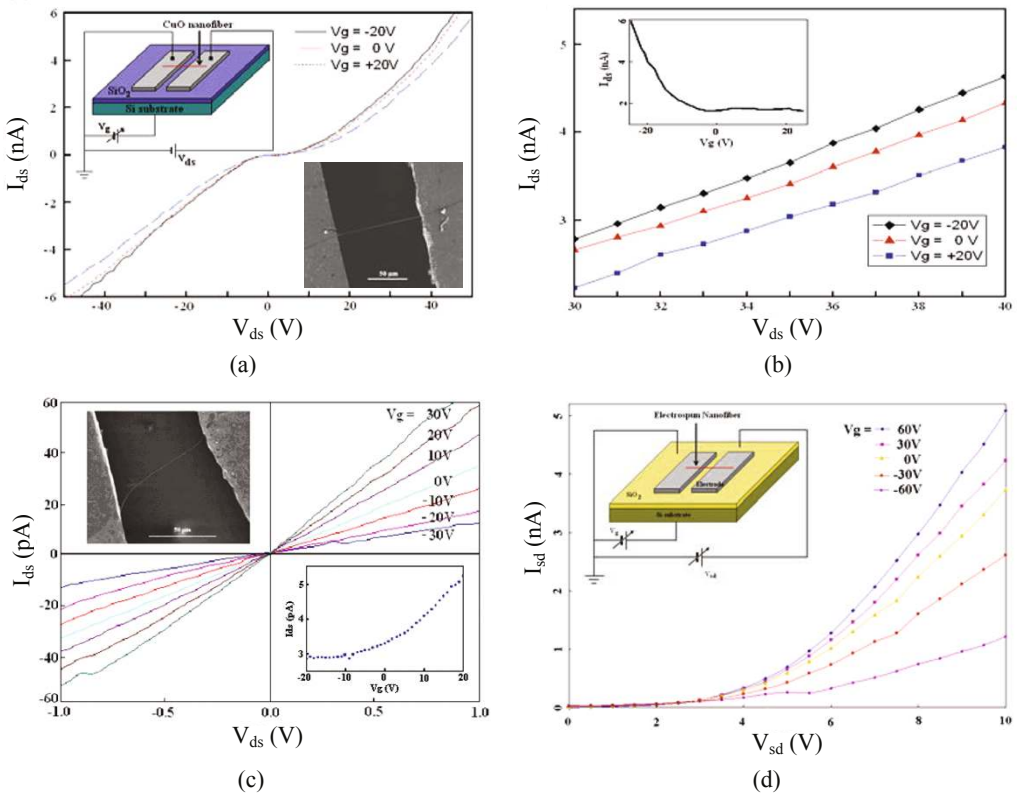

Fig. 9 (a) Gate-dependent I–V measurement of a single CuO nanofiber contacted with Ag electrodes. Measurements were done at room temperature. Upper inset: Schematic view of a nanofiber FET configuration. The source and drain contacts are silver stripes, and heave doped p-type Si substrate serves as the back gate. Bottom inset: FE-SEM image of a 60 nm diameter CuO nanofiber with a length of ~ 100 μm suspending across the silver electrodes. (b) Enlarged plot of (a). Inset: Current Ids vs gate voltage Vg at V_{ds} = 0 V. (c) Gate-dependent I–V measurement of a single ZnO nanofiber. (d) Gate-dependent I–V measurement of a single GaN nanofiber contacted with Ag electrodes [35,43,50]. Panel a and b reprinted with permission from Wu H, Lin D D, Pan W. Appl Phys Lett 2006; 89, 133125. Copyright 2006 American Institute of Physics. Panel c reprinted with permission from Wu H, Lin D D, Zhang R, Pan W, J. Am. Ceram. Soc. 2008; 91: 656-659. Copyright 2007 The American Ceramic Society. Panel d reprinted with permission from Wu H, Lin D D, Zhang R, Zhang C. Pan W, Adv. Mater. 2009; 21: 227-231. Copyright 2009 WILEY-VCH Verlag GmbH & Co. KGaA, Weinheim

step) are shown in Fig. 9d. The current versus source-drain voltage and gate voltage were measured, the nanofiber conductance increases for Vg greater than zero and decreases for Vg less than zero, which indicates that these nanofibers are intrinsic n-type. This n-type behavior in nominally undoped GaN is believed to be attributed to the nitrogen vacancies and/or oxygen impurities [50].

Our results indicated that semiconductive ceramic nanofibers can be directly assembled into FETs using the simple and versatile electrospinning method. The nanofiber transistors should be useful in building low-cost logic and switching circuits, as well as highly sensitive chemical and biological sensors with reduced device dimensions.

It is of great interest to study oxide nanofibers with doping of selection of elements for enhancing and controlling their mechanical, electrical, and optical performance. Our group studied the electrical properties of single aluminum-doped zinc oxide nanofibers [16]. Typical current–voltage (I–V) curve through a single AZO nanowire with different Al concentrations is shown in Fig. 10, and the corresponding conductivity was calculated (Fig. 10). Compared to the pure ZnO nanowire with a conductivity of 2.55×10^{-5} S cm^{-1}, the Al-doped ZnO nanowires show a steep increase up to 9.73×10^{-3} S cm^{-1} (Al = 5 at %), indicating a great enhancement in conductivity. Here, aluminum acts as a cationic dopant in the ZnO lattice, that is, the trivalent Al^{3+} ion will occupy the divalent Zn^{2+} site allowing electrons to move to the conduction band easily. This gives a net increase in the concentration of electrons, thereby enhancing the electrical conductivity [16]. Lin *et al.* studied electrical transfer properties of indium doped tin oxide (ITO) nanofibers [37]. Devices for I–V measurement and field-effect transistors (FETs) were assembled using ITO nanowires with top contact configurations. The effect of Sn doping on the electrical conductivity was significant in that it enhanced the conductance by over 10^7 times, up to ~1 S cm^{-1} for ITO nanowires with an Sn content of 17.5 at.%. The nanowire FETs were operated in the depletion mode with an electron mobility of up to 0.45 cm^2 V^{-1} s^{-1} and an on/off ratio of 10^3.

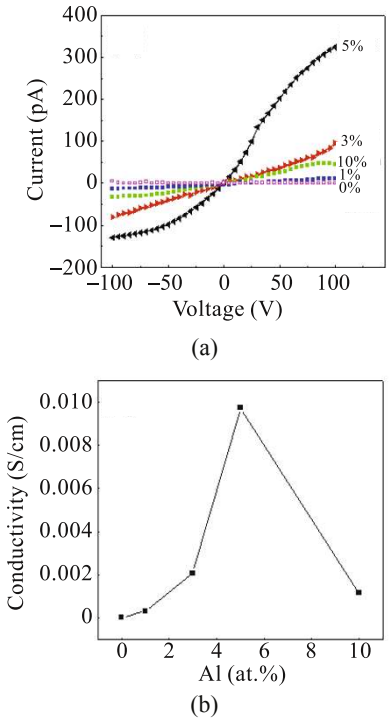

Fig. 10 (a) The measured current–voltage (I–V) curves of undoped and Al-doped samples; (b) Al at % dependent conductivity of AZO nanowires [16]. Reprinted with permission from Lin D, Wu H, Pan W. Advanced Materials 2007; 19: 3968-3972. Copyright 2007 WILEY-VCH Verlag GmbH & Co. KGaA, Weinheim

5.2 Optical properties and photo sensors

Electrospun inorganic nanofibers have interesting optical properties due to its shrinked dimensions and nanoscale grain sizes. For example, our group studied the photoluminescence (PL) spectroscopy of electrospun GaN nanofibers [50]. Spectra were collected at room temperature, exited by a monochromatic source with excitation energy of 3.82 eV (325 nm). The PL spectrum (Fig. 11a) from GaN nanofibers showed a broad peak at 363 nm (3.42 eV), and a small, narrow peak at 333 nm (3.72 eV). It is known that the size effect widens the bandgap of nanowires and that a blue-shift may occur to the PL spectrum; however, surface effects narrow the bandgap of nanowires. According to our experimental results, the primary bandgap of the nanofibers (3.42 eV) is a little higher than that reported for bulk GaN (Wurtzite: 3.4 eV), which indicates a combination of the size effect and surface effect. As ammonia exists during the fabrication of GaN nanowires, surface passivation of GaN nanowires may exist, and accordingly modifies the bandgap, as reported for other nitride nanowires. The small peak at 333 nm demonstrated a blue-shift in the emission photon energy of the nanoparticles compared with the bandgap of bulk GaN, which shows that the emission peak is a result of the quantum

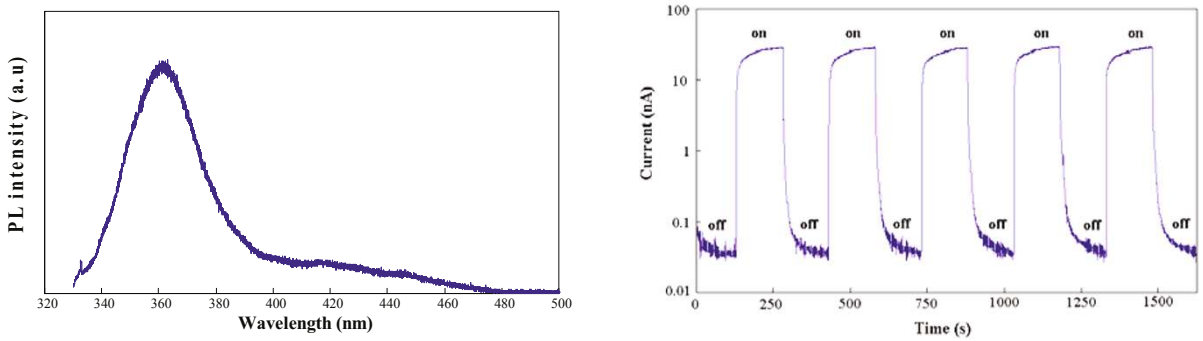

(a) (b)

Fig. 11 (a) Room temperature PL spectrum of GaN nanofibers. The excitation wavelength is 325 nm from a He-Cd laser. (b) Conductance response of a GaN nanofiber upon pulsed illumination from a 254 nm wavelength UV light with a power density of 3 $Mwcm^{-2}$ [50]. Reprinted with permission from Wu H, Lin D D, Zhang R, Zhang C. Pan W, Adv. Mater. 2009; 21: 227-231. Copyright 2009 WILEY-VCH Verlag GmbH & Co. KGaA, Weinheim

confined states in GaN nanoparticles. Considering the wide direct band gap, nanometer-scale dimensions, and also taking advantage of the high aspect ratio and rough surfaces, electrospun ceramic nanofibers are suitable for ultraviolet photodetection applications [50]. Figure 11b shows the photoconductance response of the GaN nanofiber FET device fabricated by Wu *et al*. The measured Isd of the nanofiber device showed a rapid increase from about 0.03 to 25 nA upon exposure. The electrospun GaN nanofibers show much higher sensitivity to UV detection than that of single crystalline GaN nanowires. From their measurement data, the conductance of an electrospun GaN nanofiber increases by 830 times when UV was on. In contrast, a single crystal GaN nanowire grown by the chemical vapour deposition (CVD) method showed a smaller response (~78) to UV light [50]. A similar enhancement of photoresponse within electrospun ceramic nanofibers has also been demonstrated in Ag/ZnO and AZO material systems. For example, photoactive material consisting of heterogeneous Ag–ZnO nanowires and nanofibers was prepared by electrospinning by Lin *et al*. Tunable UV photodetectors fabricated using Ag–ZnO NWs have shown high sensitivity up to over four orders of magnitude with relatively fast and stable response speed (Fig. 12) [48]. In conclusion, electrospun nanofibers is suitable for assembling next generation high-performance photo-sensor devices due to its unique polycrystalline nature and rough surfaces, which lead to a high surface area-to-volume ratio, and subsequently result in more photo generated carriers compared with a smooth single crystalline nanowires.

5.3 Memory device

Electrospun ceramic nanofibers have been assembled to functional nano-scale smart electronic devices including but not limited to FETs and sensors. Lin *et al.* developed single ZnO nanofiber based memories. A nanoscale memory device constructed from an individual AZO nanowire was observed to switch between two states differing in conductivity by about one order of magnitude, because of field-induced charge trapping and de-trapping (Fig. 13) [16]. These results demonstrate that multifunctional AZO nanostructures prepared by electrospinning have great potential applications in next-generation semiconductor devices, such as diodes and photodetectors, as well as transparent sensors and memories.

5.4 Magnetic properties

Magnetic properties of ceramic nanofiber systems have been widely studied [55,61,89-93]. For example, Fe-doped TiO_2-SnO_2 hybrid nanofiber has been prepared via electrospinning method. The magnetic property versus Fe doping content was characterized[55]. The magnetic properties have also been characterized for the Fe-TiO_2/SnO_2 nanofibers before and after annealing under vacuum atmosphere, and nanofibers show obvious ferromagnetic property at room temperature as they are annealed (Fig. 14a) [55]. Wu *el al.* showed that the simple solution-based electrospinning synthetic method allows convenient assembly and precise doping of Mn or other elements into the GaN nanofiber matrix and the Mn-doped GaN

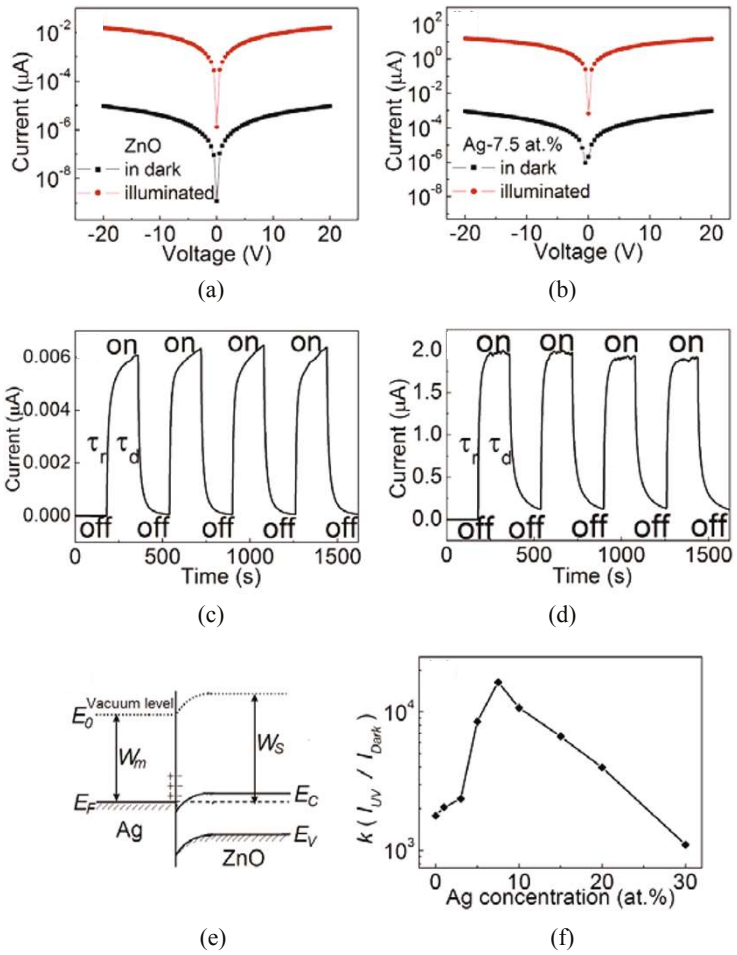

Fig. 12 Typical I–V characteristics of dark current and photocurrent through individual nanowires under UV illumination λ=254 nm: (a) ZnO; (b) 7.5 at. % Ag-ZnO. Time-dependent photore sponses at a bias voltage of 4 V: (c) ZnO; (d) 7.5 at. % Ag-ZnO. (e) Proposed schematic illustrations of the energy band structure of the Ag-ZnO heterostructure. (f) Dependence of photosensitivity k on Ag loadings, where k is defined as the ratio of photocurrent to dark current that measured at 4 V, respectively [48]. Reprinted with permission from Lin D D, Wu H, Zhang W, *et al*. Appl Phys Lett 2009; 94: 172103. Copyright 2006 American Institute of Physics

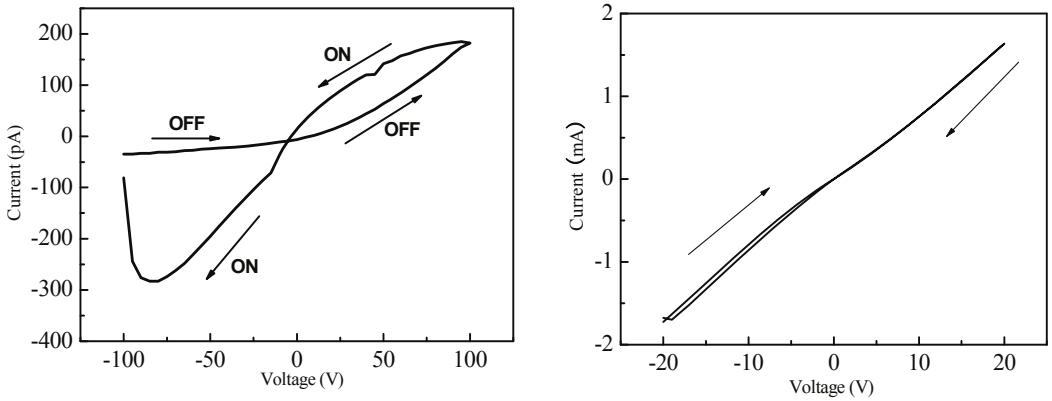

Fig. 13 (a) Memory characteristics of the AZO nanowires (Al at %=3 %). (b) Current–voltage (I–V) curves of the AZO film with 200 nm thickness. Reprinted with permission from Lin D, Wu H, Pan W. Advanced Materials 2007; 19: 3968-3972. Copyright 2007 WILEY-VCH Verlag GmbH & Co. KGaA,Weinheim

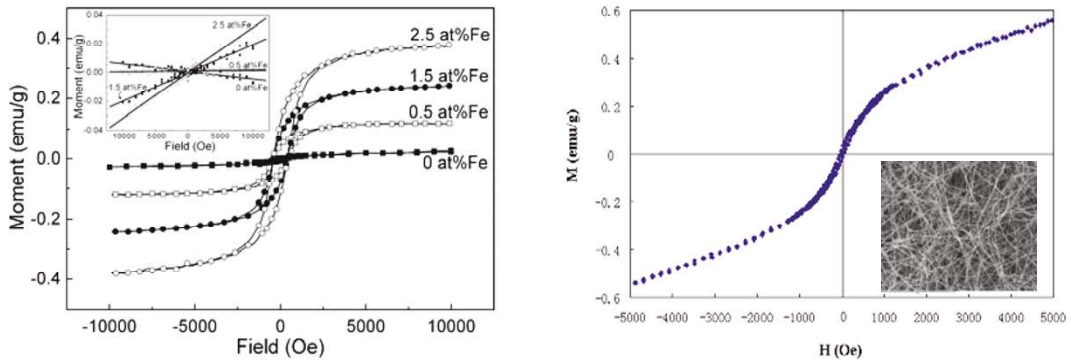

(a) (b)

Fig. 14 (a) Magnetic hysteresis loops of Fe-TiO_2/SnO_2 hybrid nanofibers after vacuum annealing. Inset shows the magnetic property of them before vacuum annealing [55]. (b) Magnetization loops of the nanofibers measured at room temperature. Inset shows a typical SEM image of the samples. Scale bar is 1μm [50]. Panel a reprinted with permission from Zhang R, Wu H, Lin DD, *et al*. J Am Ceram Soc 2010; 93: 605-608. Copyright 2009 The American Ceramic Society. Panel b reprinted with permission from Wu H, Lin D D, Zhang R, Zhang C. Pan W, Adv. Mater. 2009; 21: 227-231. Copyright 2009 WILEY-VCH Verlag GmbH & Co. KGaA,Weinheim

nanofibers show ferromagnetic character at room temperature (Fig. 14b) [50]. Their result shows a new way to the facile synthesis of diluted magnetic semiconductor (DMS) nanofibers, which is of significant importance for constructing spintronic nanodevices such as ultrasensitive magnetic field sensors and spin FETs.

5.5 Phase transition

Nano-structured ceramics are also suggested to have different thermal stabilities compared with their bulks due to the shrinked dimensions and size effects. Our group studied the phase stability of ferroelectric and piezoelectric ceramic nanofibers. $BaTiO_3$ nanofibers with diameters ranging from 92 to 182 nm have been prepared by electrospinning [45]. XRD and SEM revealed that when the annealing temperature is higher than 600 ℃, completely crystallized $BaTiO_3$ nanofibers could be obtained and the grain size almost kept a constant value (~13.7 nm) when the annealing time lasted longer than 8 h at 600 ℃. Besides, the diameters of fibers decreased when the annealing temperature increased from 500 to 600 ℃, but at elevated temperature higher than 600 ℃, the fibers became thicker and also exhibited a rougher surface feature. Tetragonal to cubic phase transition in BTO nanofibers were monitored using Raman spectroscopy (Fig. 15). They found that the electrospun $BaTiO_3$ nanofibers have much higher Tc (~220 ℃) than bulk $BaTiO_3$ ceramics (~130 ℃) [45]. This effect can be understood by considering the shrinked sizes in $BaTiO_3$ nanofibers. The reduced grain size in electrospun $BaTiO_3$ nanofibers caused larger grain-boundary areas, and further relieved internal stresses in materials due to grain-boundary sliding. Smaller internal stresses, relaxed by grain boundaries, could decrease the free energy of the ferroelectric phase, and thus increase the Curie temperature. Our research indicates that electrospinning ceramic nanofibers may have different phase stability of ceramics than in bulks, which provides an exciting opportunity for controlling the electrical, optical and ferroelectric performance of ceramics.

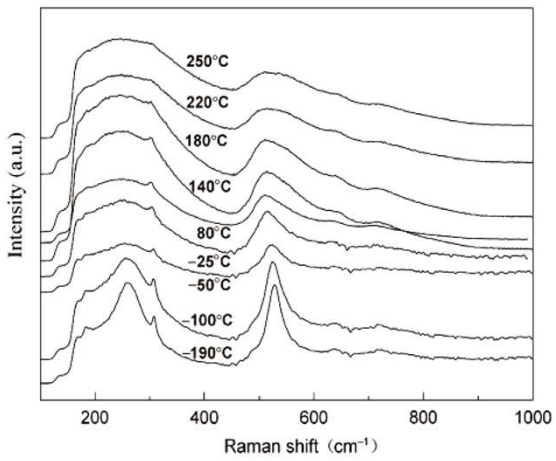

Fig. 15 Raman spectra of $BaTiO_3$ nanofibers at various temperatures [45]. Reprinted with permission from Li H P, Wu H, Lin D D, *et al*. J Am Ceram Soc 2009; 92: 2162-2164. Copyright 2009 The American Ceramic Society

5.6 Energy storage

Electrospinning ceramic nanofiber, which has extremely high surface area according to its small size and provides fast charge-transfer channels along its 1D nanostructure, has been considered as an ideal material system for energy storage applications [94-138]. For example, Mai *et al.* demonstrated high performance lithium ion battery electrode based on electrospun vanadium oxide nanofibers [133]. They prepared ultralong hierarchical vanadium oxide nanowires with diameter of 100-200 nm and length up to several millimeters using the low-cost starting materials by electrospinning combined with annealing. The hierarchical nanowires were constructed from attached vanadium oxide nanorods of diameter around 50 nm and length of 100 nm. The initial and 50th discharge capacities of the ultralong hierarchical vanadium oxide nanowire cathodes are up to 390 and 201 mAh/g when the lithium ion battery cycled between 1.75 and 4.0 V (Fig. 16). When the battery was cycled between 2.0 and 4.0 V, the initial and 50th discharge capacities of the nanowire cathodes are 275 and 187 mAh/g. Compared with self-aggregated short nanorods synthesized by hydrothermal method, the ultralong hierarchical vanadium oxide nanowires exhibit much higher capacity. This is due to the fact that self-aggregation of the unique nanorod-in-nanowire structures has been greatly reduced because of the attachment of nanorods in the ultralong nanowires, which can keep the effective contact areas of active materials, conductive additives, and electrolyte large and fully realize the advantage of nanomaterial-based cathodes. This demonstrates that ultralong hierarchical vanadium oxide nanowire is one of the most favorable nanostructures as cathodes for improving cycling performance of lithium ion batteries [133].

5.7 Photo catalyst

Environmental problems such as air and water pollution have provided the impetus for sustained fundamental and applied research in the area of environmental remediation [139-144]. With the steady and fast growing field of nanoscience and nanotechnology, nanostructured ceramics like zinc oxide and titanium oxide has become a promising photocatalyst for its high catalytic activity, low cost, and environmental friendliness [50,51,55,57,

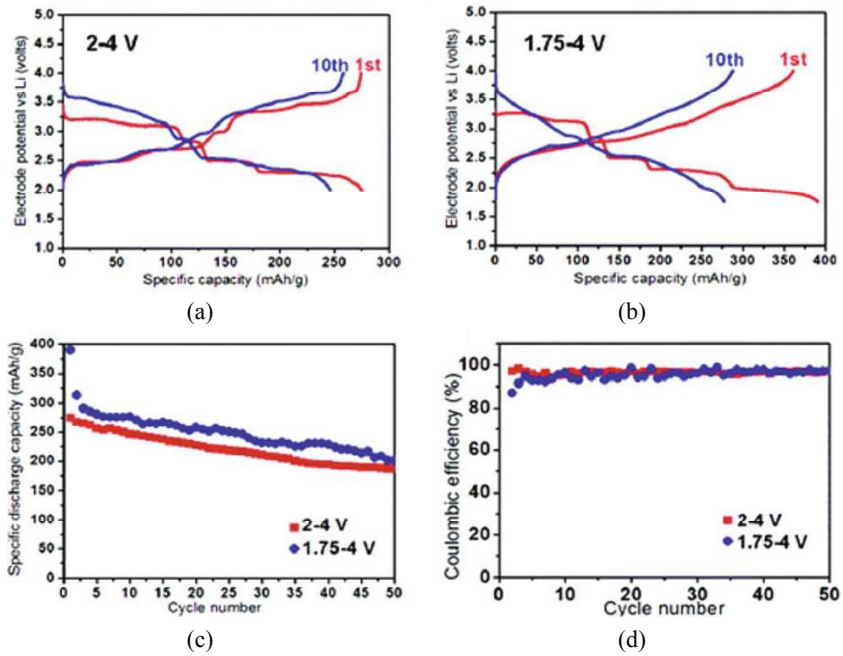

Fig. 16 (a), (b) Charge/discharge curves of hierarchical vanadium oxide nanowires at voltages of 2-4 and 1.75-4 V, respectively. (c), (d) Capacity vs cycle number, and Coulombic efficiency vs cycle number of the ultralong hierarchical vanadium oxide nanowires [133]. Reprinted with permission from Mai L Q, Xu L, Han C H, *et al*. Nano Lett 2010; 10: 4750-4755. Copyright 2010 American Chemical Society

139-142,145-152]. Major limitation of achieving high photocatalytic efficiency in the ceramic nanostructure systems is the quick recombination of charge carriers. Electrospinning ceramic nanofibers have extremely high surface area due to its small sizes, and further provide channels for quick charge transfer due to its 1D nanostructures. Therefore, electrospun ceramics have huge potential for photo catalyst applications [47, 57,145-155]. Our group fabricated photocatalytically active Ag-ZnO composite nanofibers by electrospinning (Fig. 17) [47]. The resultant heterostructure could promote the charge separation of the photogener ated electrons (e-) and holes (h+), allowing both of the e- and h+ participating in the overall photocatalytic reaction. The optimal photocatalytic activity of Ag-ZnO nanofibers exceeded that of pure ZnO nanofibers by a factor of more than 25 when the Ag concentration was kept at 7.5 atom %. Therefore, exploring the catalytic activity of such composite structures may pave the way for designing useful nanoscale building blocks for photocatalytic and photovoltaic applications [47]. Zhang *et al.* synthesized hybrid Fe-TiO_2/SnO_2 nanofibe with combination of high photocatalytic activity and room temperature ferromagnetic properties. It is believed that this hybrid nanofiber may serve as a candidate of new generation of visible light-excitable photocatalyst, which is also possibly easy for recycling and its potential applications are foreseeable in some fields such as water purifying and pollution treatment [55].

5.8 Filters and separators

Taking advantages of the highly porous fibrous nanostructures, ceramic nanofiber membrane can be used for filter and separator applications [128,156-159]. For example, Ke *et al.* demonstrate high performance filters by constructing a hierarchically structured

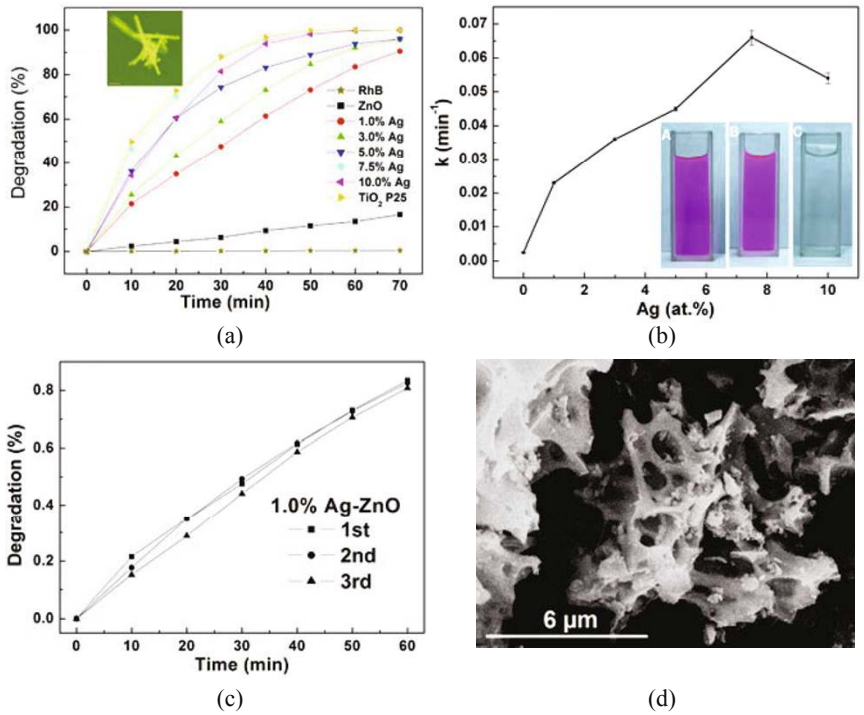

Fig. 17 (a) Kinetics of the photodegradation of an aqueous solution of RhB by Ag-ZnO heterojunction nanofibers. The inset was the typical morphology of the photocatalyst dispersed in the dye solution (scale bar: 5 μm). (b) Degradation rate constants for Ag-ZnO nanofibers obtained in the presence of different Ag contents (the inset illustrates photos for comparison of the RhB solutions photodegraded with various Ag-ZnO nanofibers for 70 min; A, without catalyst; B, pure ZnO; and C, 7.5 atom% Ag-ZnO). (c) The repeatability tests studied on the 1.0 atom% Ag-ZnO sample for three recycles. (d) The SEM image of the sample reclaimed after photocatalytic measurement [47]. Reprinted with permission from Lin D D, Wu H, Zhang R, Pan W, Chem. Mater. 2009; 21: 3479-3484. Copyright 2009 American Chemical Society

separation layer on a porous substrate using large titanate nanofibers and smaller boehmite nanofibers [157]. Traditional ceramic separation membranes, which are fabricated by applying colloidal suspensions of metal hydroxides to porous supports, tend to suffer from pinholes and cracks that seriously affect their quality. Other intrinsic problems for these membranes include dramatic losses of flux when the pore sizes are reduced to enhance selectivity and dead-end pores that make no contribution to filtration. Electrospun ceramic nanofiber mats can successfully overcome these challenges. The ceramic nanofibers are able to divide large voids into smaller ones without forming dead-end pores and with the minimum reduction of the total void volume. The separation layer of nanofibers has a porosity of over 70% of its volume, whereas the separation layer in conventional ceramic membranes has a porosity below 36% and inevitably includes deadend pores that make no contribution to the flux. This radical change in membrane texture greatly enhances membrane performance. The resulting membranes were able to filter out 95.3% of 60-nm particles from a 0.01 wt % latex while maintaining a relatively high flux of between 800 and 1000 L/(m^2·h), under a low driving pressure (20 kPa). Such flow rates are orders of magnitude greater than those of conventional membranes with equal selectivity. Moreover, the flux was stable at approximately 800 L/(m^2·h) with a selectivity of more than 95%, even after six repeated runs of filtration and calcination. Use of different supports, either porous glass or porous alumina, had no substantial effect on the performance of the membranes; thus, it is possible to construct the membranes from a variety of supports without compromising functionality. The Darcy equation satisfactorily describes the correlation between the filtration flux and the structural parameters of the new membranes. The assembly of nanofiber meshes to combine high flux with excellent selectivity is an exciting new direction in membrane fabrication.

6 Conclusions and future perspective

Electrospun nanofibers are extremely long. Such high-aspect-ratio nanofibers made of ceramics provide an exciting materials system to investigate some fundamentally important problems, especially electrical, mechanical, magnetic and optical phenomena at the nanometer scale in ceramic science. Most ceramic nanofibers prepared by electrospinning are polycrystalline, which is quite different from CDV-grown single crystalline inorganic nanowires. The grain or domain size can be comparable with the diameter of the fibers, and may further provide unique functions like modified phase stability and high sensitivity to environmental. The electrospun nanofibers can be easily assembled for device integrations, which is important for future smart electronic devices in nanoscale. Another obvious advantage for electrospinning ceramic nanofibers is that the fabrication process is highly efficient and scalable. The low cost electrospun nanofibers hold potential for applications in photocatalyst and lithium ion battery electrodes. As both electrospinning and sol-gel processing techniques are being constantly improved, it is expected that progress in understanding the properties and applications of ceramic nanofibers will be accelerated in the coming years.

Acknowledgment

This study was supported by the National Natural Science Foundation of China (Nos. 50872063, 50990302, and 51072088).

References

[1] Palacios T. Applied physics nanowire electronics comes of age. *Nature* 2012, **481**: 152-153.

[2] Yan H, Choe HS, Nam SW. Programmable nanowire circuits for nanoprocessors. *Nature* 2011, **470**: 240-244.

[3] Yaman M, Khudiyev T, Ozgur E, *et al*. Arrays of indefinitely long uniform nanowires and nanotubes. *Nat Mater* 2011, **10**: 494-501.

[4] Tsivion D, Schvartzman M, Popovitz-Biro R, *et al*. Guided growth of millimeter-long horizontal nanowires with controlled orientations. *Science* 2011, **333**: 1003-1007.

[5] Huang JY, Li Z, Chong MW, *et al*. In situ observation of the electrochemical lithiation of a single SnO_2 nanowire electrode. *Science* 2010, **330**: 1515-1520.

[6] Tian BZ, Zheng XL, Kempa T, *et al.* Coaxial silicon nanowires as solar cells and nanoelectronic power sources. *Nature* 2007, **449**: 885-889.

[7] Gao PX, Ding Y, Mai WJ, *et al*. Conversion of zinc oxide nanobelts into superlattice-structured nanohelices. *Science* 2005, **309**: 1700-1704.

[8] Ju SY, Facchetti A, Xuan Y, *et al*. Fabrication of fully transparent nanowire transistors for transparent and flexible electronics. *Nat Nanotechnol* 2007, **2**: 378-384.

[9] Huang Y, Duan XF, Wei QQ, *et al*. Directed assembly of one-dimensional nanostructures into functional networks. *Science* 2001, **291**: 630-633.

[10] Law M, Goldberger J, Yang P D. Semiconductor nanowires and nanotubes. *Ann Rev Mater Res* 2004, **34**: 83-122.

[11] Limmer SJ, Seraji S, Wu Y, *et al*. Template-based growth of various oxide nanorods by sol-gel electrophoresis. *Adv Funct Mater* 2002, **12**: 59-64.

[12] Varghese OK, Grimes CA. Metal oxide nanoarchitectures for environmental sensing. *J Nanosci Nanotechnol* 2003, **3**: 277-293.

[13] Kuchibhatla S, Karakoti AS, Bera D, *et al*. One dimensional nanostructured materials. *Prog Mater Sci* 2007, **52**: 699-913.

[14] Lu XF, Wang C, Wei Y. One-dimensional composite nanomaterials: synthesis by electrospinning and their applications. *Small* 2009, **5**: 2349-2370.

[15] Li Y, Qian F, Xiang J. *et al*. Nanowire electronic and optoelectronic devices. *Mater Today* 2006, **9**: 18-27.

[16] Lin D, Wu H, Pan W. Photoswitches and memories assembled by electrospinning aluminum-doped zinc oxide single nanowires. *Advanced Materials* 2007, **19**: 3968-3972.

[17] Lieber CM. One-dimensional nanostructures: Chemistry, physics & applications. *Solid State Comm* 1998, **107**: 607-616.

[18] Xia YN, Yang PD, Sun YG, *et al*. One-dimensional nanostructures: Synthesis, characterization, and applications. *Adv Mater* 2003, **15**: 353-389.

[19] Chan CK, Peng H, Liu G, *et al*. High-performance lithium battery anodes using silicon nanowires. *Nat Nanotechnol* 2008, **3**: 31-35.

[20] Li YG, Tan B, Wu YY. Mesoporous CO_3O_4 nanowire arrays for lithium ion batteries with high capacity and rate capability. *Nano Lett* 2008, **8**: 265-270.

[21] Martin CR. Membrane-based synthesis of nanomaterials. *Chem Mater* 1996, **8**: 1739-1746.

[22] Hulteen JC, Martin CR. A general template-based method for the preparation of nanomaterials. *J Mater Chem* 1997, 7: 1075-1087.

[23] Dresselhaus, MS, Chen G, Tang MY, *et al*. New directions for low-dimensional thermoelectric materials. *Adv Mater* 2007, **19**: 1043-1053.

[24] McCann JT, Li D, Xia YN. Electrospinning of nanofibers with core-sheath, hollow, or porous structures. *J Mater Chem* 2005, **15**: 735-738.

[25] Sigmund W, Yuh J, Park H, *et al*. Processing and structure relationships in electrospinning of ceramic fiber systems. *J Am Ceram Soc* 2006, **89**: 395-407.

[26] Ramaseshan R, Sundarrajan S, Jose R, *et al*. Nanostructured ceramics by electrospinning. *J Appl Phys* 2007, **102**: 111101-111117.

[27] Li D, Xia YN. Electrospinning of nanofibers: Reinventing the wheel? *Adv Mater* 2004, **16**: 1151-1170.

[28] Teo WE, Ramakrishna S. A review on electrospinning design and nanofibre assemblies. *Nanotechnol* 2006, **17**: R89-R106.

[29] Li D, Wang YL, Xia YN. Electrospinning of polymeric and ceramic nanofibers as uniaxially aligned arrays. *Nano Lett* 2003, **3**: 1167-1171.

[30] Li D, McCann JT, Xia YN. Electrospinning: A simple and versatile technique for producing ceramic nanofibers and nanotubes. *J Am Ceram Soc* 2006, **89**: 1861-1869.

[31] Dersch R, Graeser M, Greiner A, *et al*. Electrospinning of nanofibres: Towards new techniques, functions, and applications. *Aust J Chem* 2007, **60**: 719-728.

[32] Li D, Xia YN. Fabrication of titania nanofibers by electrospinning. *Nano Lett* 2003, **3**: 555-560.

[33] Li D, Wang YL, Xia YN. Electrospinning nanofibers as uniaxially aligned arrays and layer-by-layer stacked films. *Adv Mater* 2004, **16**: 361-366.

[34] Li D, Xia YN. Direct fabrication of composite and ceramic hollow nanofibers by electrospinning.

Nano Lett 2004, **4**: 933-938.

[35] Wu H, Lin D, Pan W. Fabrication, assembly, and electrical characterization of CuO nanofibers. *Appl Phys Lett* 2006, **89**: 133125.

[36] Wu H, Pan W. Preparation of zinc oxide nanofibers by electrospinning. *J Am Ceram Soc* 2006, **89**: 699-701.

[37] Lin D, Wu H, Zhang R, *et al*. Preparation and electrical properties of electrospun tin-doped indium oxide nanowires. *Nanotechnol* 2007, **18**: 465301.

[38] Lin D, Wu H, Zhang R, *et al*. Preparation of ZnS nanofibers via electrospinning. *J Am Ceram So* 2007, **90**: 3664-3666.

[39] Lin D, Pan W, Wu H. Morphological control of centimeter long aluminum-doped zinc oxide nanofibers prepared by electrospinning. *J Am Ceram Soc* 2007, **90**: 71-76.

[40] Lin D, Wu H, Pan W. Preparation of Eu, Li Co-doped ZnO red fluorescence nanofibers by electrospinning and their characterization. *Rare Metal Mater Eng* 2007, **36**: 220-222.

[41] Wu H, Lin D, Zhang R, *et al*. Oriented nanofibers by a newly modified electrospinning method. *J Am Ceram Soc* 2007, **90**: 632-634.

[42] Wu H, Zhang R, Liu XX, *et al*. Electrospinning of Fe, Co, and Ni nanofibers: Synthesis, assembly, and magnetic properties. *Chem Mater* 2007, **19**: 3506-3511.

[43] Wu H, Lin D, Zhang R, *et al*. ZnO nanofiber field-effect transistor assembled by electrospinning. *J Am Ceram Soc* 2008, **91**: 656-659.

[44] Wu H, Zhang R, Sun Y, *et al*. Biomimetic nanofiber patterns with controlled wettability. *Soft Matter* 2008, **4**: 2429-2433.

[45] Li HP, Wu H, Lin DD, *et al*. High T_c in electrospun $BaTiO_3$ nanofibers. *J Am Ceram Soc* 2009, **92**: 2162-2164.

[46] Li HP, Wu H, Pan W. Preparation of $BaTiO_3$ nanofibers via electrospinning. *Rare Metal Mater Eng* 2009, **38**: 994-996.

[47] Lin D, Wu H, Zhang R, *et al*. Enhanced photocatalysis of electrospun Ag-ZnO heterostructured nanofibers. *Chem Mater* 2009, **21**: 3479-3484.

[48] Lin D, Wu H, Zhang W, *et al*. Enhanced UV photoresponse from heterostructured Ag-ZnO nanowires. *Appl Phys Lett* 2009, **94**: 172103.

[49] Qin XL, Wu H, Lin DD, *et al*. Preparation of ZnO nanofibers with high specific surface area. *Rare Metal Mater Eng* 2009, **38**: 997-999.

[50] Wu H, Sun Y, Lin D, *et al*. GaN nanofibers based on electrospinning: Facile synthesis, controlled assembly, precise doping, and application as high performance UV photodetector. *Adv Mater* 2009, **21**: 227-231.

[51] Zhang R, Wu H, Lin D, *et al*. Preparation of necklace-structured TiO_2/SnO_2 hybrid nanofibers and their photocatalytic activity. *J Am Ceram Soc* 2009, **92**: 2463-2466.

[52] Zhang R, Wu H, Lin D, *et al*. $LaMnO_3$ and $La_{0.875}Sr_{0.125}MnO_3$ nanofibers via electrospinning. *Rare Metal Mater Eng* 2009, **38**: 1000-1002.

[53] Li HP, Sun Y, Zhang W, *et al*. Preparation of heterostructured $Ag/BaTiO_3$ nanofibers via electrospinning. *J Alloys Comp* 2010, **508**: 536-539.

[54] Li HP, Zhang W, Li B, *et al*. Diameter-dependent photocatalytic activity of electrospun TiO_2 nanofiber. *J Am Ceram Soc* 2010, **93**: 2503-2506.

[55] Zhang R, Wu H, Lin D, *et al*. Photocatalytic and magnetic properties of the $Fe\text{-}TiO_2/SnO_2$ nanofiber via electrospinning. *J Am Ceram Soc* 2010, **93**: 605-608.

[56] Li HP, Zhang W, Pan W. Enhanced photocatalytic activity of electrospun TiO_2 nanofibers with optimal anatase/rutile ratio. *J Am Ceram Soc* 2011, **94**: 3184-3187.

[57] Lin D, Wu H, Zhang R, *et al*. Facile synthesis of heterostructured ZnO-ZnS nanocables and enhanced photocatalytic activity. *J Am Ceram Soc* 2010, **93**: 3384-3389.

[58] Wu H, Lin D, Pan W. High performance surface-enhanced Raman scattering substrate combining low dimensional and hierarchical nanostructures. *Langm* 2010, **26**: 6865-6868.

[59] Huang ZM, Zhang YZ, Kotaki M, *et al*. A review on polymer nanofibers by electrospinning and their applications in nanocomposites. *Comp Sci Technol* 2003, **63**: 2223-2253.

[60] Pham QP, Sharma U, Mikos AG. Electrospinning of polymeric nanofibers for tissue engineering applications: A review. *Tissue Eng* 2006, **12**: 1197-1211.

[61] Li D, Herricks T, Xia YN. Magnetic nanofibers of nickel ferrite prepared by electrospinning. *Appl*

Phys Lett 2003, **83**: 4586-4588.

[62] Kim JK, Chauhan GS, Ahn JH, *et al*. Effect of synthetic conditions on the electrochemical properties of $LiMn_{0.4}Fe_{0.6}PO_4$/C synthesized by sol-gel technique. *J Power Sources* 2009, **189**: 391-396.

[63] Lee SH, Jung M, Im JS, *et al*. Preparation and characterization of electrospun LiFePO(4)/carbon complex improving rate performance at high C-rate. *Res Chem Intermed* 2010, **36**: 591-602.

[64] Lu HW, Yu L, Zeng W, *et al*. Fabrication and electrochemical properties of three-dimensional structure of LiCoO fibers. *Electrochem Solid State Lett* 2008, **11**: A140-A144.

[65] Zhan SH, Li Y, Yu HB. $LiCoO_2$ hollow nanofibers by co-electrospinning sol-gel precursor. *J Dispersion Sci Technol* 2008, **29**: 702-705.

[66] Gu YX, Chen DR, Jiao ML. Synthesis and electrochemical properties of nanostructured $LiCoO_2$ fibers as cathode materials for lithium-ion batteries. *J Phys Chem B* 2005, **109**: 17901-17906.

[67] Shao CL, Yu N, Liu YC, Preparation of $LiCoO_2$ nanofibers by electrospinning technique. *J Phys Chem Solids* 2006, **67**: 1423-1426.

[68] Fu ZW, Ma J, Qin QZ. Nanostructured $LiCoO_2$ and $LiMn_2O_4$ fibers fabricated by a high frequency electrospinning. *Solid State Ionics* 2005, **176**: 1635-1640.

[69] Shao CL, Guan HY, Wen SB, *et al.* A novel method for making NiO nanofibres via an electrospinning technique. *Chin Chem Lett* 2004, **15**: 365-367.

[70] Moon J, Park JA, Lee SJ, *et al*. Structure and electrical properties of electrospun Zno-NiO mixed oxide nanofibers. *Current ApplPhys* 2009, **9**: S213-S216.

[71] Guan HY, Shao CL, Wen SB, *et al.* Preparation and characterization of NiO nanofibres via an electrospinning technique. *Inorg Chem Comm* 2003, **6**: 1302-1303.

[72] Shao CL, Yang XH, Guan HY, *et al*. Electrospun nanofibers of NiO/ZnO composite. *Inorg Chem Comm* 2004, **7**: 625-627.

[73] Fan Q, Whittingham MS. Electrospun manganese oxide nanofibers as anodes for lithium-ion batteries. *Electrochem Solid State Lett* 2007, **10**: A48-A51.

[74] Zhan SH, Chen DR, Jiao XL, *et al*. Facile fabrication of long α-Fe_2O_3, α-Fe and γ-Fe_2O_3 hollow fibers using sol-gel combined co-elecrospinning technology. *J Colloid Interf Sci* 2007, **308**: 265-270.

[75] Zhu Y, Zhang JC, Zhai J, *et al*. Preparation of superhydrophilic α-Fe_2O_3 nanofibers with tunable magnetic properties. *Thin Solid Films* 2006, **510**: 271-274.

[76] Park SJ, Bhargava S, Bender ET, *et al*. Palladium nanoparticles supported by alumina nanofibers synthesized by electrospinning. *J Mate Res* 2008, **23**: 1193-1196.

[77] Yang XH, Shao CL, Liu YC. Fabrication of Cr_2O_3/Al_2O_3 composite nanofibers by electrospinning. *J Mater Sci* 2007, **42**: 8470-8472.

[78] Peng Q, Sun XY, Spagnola JC, *et al*. Atomic layer deposition on electrospun polymer fibers as a direct route to Al_2O_3 microtubes with precise wall thickness control. *Nano Lett* 2007, **7**: 719-722.

[79] Rose M, Kockrick E, Senkovska I, *et al*. High surface area carbide-derived carbon fibers produced by electrospinning of polycarbosilane precursors. *Carbon* 2010, **48**: 403-407.

[80] Shin DG, Riu DH, Kim HE. Web-type silicon carbide fibers prepared by the electrospinning of polycarbosilanes. *J Ceram Process Res* 2008, **9**: 209-214.

[81] Kim SJ, Yun SM, Lee YS. Characterization of nanocrystalline porous SiC powder by electrospinning and carbothermal reduction. *J Indus Eng Chem* 2010, **16**: 273-277.

[82] Eick B, Youngblood J. SiC nanofibers by pyrolysis of electrospun preceramic polymers. *J Mater Sci* 2009, **44**: 160-165.

[83] Qiu YJ, Yu J, Rafique J, *et al*. Large-scale production of aligned long boron nitride nanofibers by multijet/multicollector electrospinning. *J Phys Chem C* 2009, **113**: 11228-11234.

[84] Cui XM, Nam YS, Lee JY, *et al*. Fabrication of zirconium carbide (ZrC) ultra-thin fibers by electrospinning. *Mater Lett* 2008, **62**: 1961-1964.

[85] Zhu PW, Hong YL, Liu BB, *et al*. The synthesis of titanium carbide-reinforced carbon nanofibers. *Nanotechnol* 2009, **20**: 255603.

[86] Kang PH, Jeun JP, Seo DK, *et al*. Fabrication of SiC mat by radiation processing. *Radia Phys Chem* 2009, **78**: 493-495.

[87] Zhang SH, Xu SZ, Dong XT, *et al*. New research progress on coaxial nanocables. *Rare Metal Mater*

Eng 2008, **37**: 1117-1123.

[88] Li D, Babel A, Jenekhe SA, *et al*. Nanofibers of conjugated polymers prepared by electrospinning with a two-capillary spinneret. *Adv Mater* 2004, **16**: 2062-2066.

[89] Xiang J, Chu YQ, Zhou GZ, *et al*. Electrospinning preparation, structural and magnetic properties of $Li_{0.5-0.5x}Zn_xFe_{2.5-0.5x}O_4$ nanofibers. *Acta Chim Sinica* 2011, **69**: 2457-2464.

[90] Nam JH, Joo YH, Lee JH, *et al*. Preparation of NiZn-ferrite nanofibers by electrospinning for DNA separation. *J Magnetism Magnetic Mater* 2009, **321**: 1389-1392.

[91] Wang ZL, Liu XJ, Lv MF, *et al.* Preparation of one-dimensional $CoFe_2O_4$ nanostructures and their magnetic properties. *J Phys Chem C* 2008, **112**: 15171-15175.

[92] Liu MQ, Shen XQ, Song FZ, *et al*. Microstructure and magnetic properties of electrospun one-dimensional Al^{3+}-substituted $SrFe_{12}O_{19}$ nanofibers. *J Solid State Chem* 2011, **184**: 871-876.

[93] Zheng W, :I ZY, Zhang HN, *et al.* Electrospinning route for α-Fe_2O_3 ceramic nanofibers and their gas sensing properties. *Mater Res Bull* 2009, **44**: 1432-1436.

[94] Cai ZY, Song J, Li JS, *et al*. Synthesis of $LiNi_{1/3}Co_{1/3}Mn_{1/3}O_2$ nanoparticles by modified Pechini method and their enhanced rate capability. *J Sol-Gel Sci Technol* 2012, **61**: 49-55.

[95] Guo BK, Li Y, Yao YF, *et al.* Electrospun $Li_4Ti_5O_{12}$/C composites for lithium-ion batteries with high rate performance. *Solid State Ionics* 2011, **204**: 61-65.

[96] Ji LW, Lin Z, Alcouttabi M, *et al*. Electrospun carbon nanofibers decorated with various amounts of electrochemically-inert nickel nanoparticles for use as high-performance energy storage materials. *Rsc Adv* 2012, **2**: 192-198.

[97] Kong JH, Liu ZL, Yang ZC, *et al*. Carbon/SnO_2/carbon core/shell/shell hybrid nanofibers: tailored nanostructure for the anode of lithium ion batteries with high reversibility and rate capacity. *Nanoscale* 2012, **4**: 525-530.

[98] Lee BS, Son SB, Park KM, *et al*. Anodic properties of hollow carbon nanofibers for Li-ion battery. *J Power Sources* 2012, **199**: 53-60.

[99] Wang HY, Gao P, Lu SF, *et al*. The effect of tin content to the morphology of Sn/carbon nanofiber and the electrochemical performance as anode material for lithium batteries. *Electrochim Acta* 2011, **58**: 44-51.

[100] Zhu PN, Wu YZ, Reddy MV, *et al*. Long term cycling studies of electrospun TiO_2 nanostructures and their composites with MWCNTs for rechargeable Li-ion batteries. *Rsc Adv* 2012, **2**: 531-537.

[101] Alcoutlabi M, Ji LW, Guo BK, *et al*. Electrospun nanofibers for energy storage. *Aatcc Review* 2011, **11**: 45-51.

[102] Cavaliere S, Subianto S, Savych I, *et al*. Electrospinning: Designed architectures for energy conversion and storage devices. *Energy Environ Sci* 2011, **4**: 4761-4785.

[103] Han H, Song T, Bae JY, *et al*. Nitridated TiO_2 hollow nanofibers as an anode material for high power lithium ion batteries. *Energy Environ Sci* 2011, **4**: 4532-4536.

[104] Ji LW, Rao MM, Aloni S, *et al*. Porous carbon nanofiber-sulfur composite electrodes for lithium/sulfur cells. *Energy Environ Sci* 2011, **4**: 5053-5059.

[105] Jung HR, Lee WJ. Electrochemical characterization of electrospun SnO(x)-embedded carbon nanofibers anode for lithium ion battery with EXAFS analysis. *J Electroanaly Chem* 2011, **662**: 334-342.

[106] Zhao G, Liu SW, Lu QF, *et al*. Preparation of Bi_2WO_6 by electrospinning: researching their synthesis mechanism and photocatalytic activity. *J Cluster Sci* 2011, **22**: 621-631.

[107] Choi HS, Kim T, Im JH, *et al*. Preparation and electrochemical performance of hyper-networked $Li_4Ti_5O_{12}$/carbon hybrid nanofiber sheets for a battery-supercapacitor hybrid system. *Nanotechnol.* 2011, **22**: 405402

[108] Doan TQ, Boyle TJ, Ottley LAM, *et al*. Synthesis, characterization, electrospinning of novel tin amide alkoxides for lithium-ion battery application. In: 241st ACS National Meeting&Exposition. Anaheim, USA, 2011.

[109] Lee JS, Kwon OS, Park SJ, *et al.* Fabrication of ultrafine metal-oxide-decorated carbon nanofibers for DMMP sensor application. *Acs Nano* 2011, **5**: 7992-8001.

[110] Roginskaya YE, Sheppelve AD, Tenchurin TK, *et al*.

Synthesis and structure of composite fibers based on silicon and carbon obtained by electrospinning. *Russ J Phys Chem A* 2011, **85**: 2013-2019.

[111] Toprakci O, Ji LW, Lin Z, *et al*. Fabrication and electrochemical characteristics of electrospun $LiFePO_4$/carbon composite fibers for lithium-ion batteries. *J Power Sources* 2011, **196**: 7692-7699.

[112] Yang XJ, Teng DH, Liu BX, *et al*. Nanosized anatase titanium dioxide loaded porous carbon nanofiber webs as anode materials for lithium-ion batteries. *Electrochem Comm* 2011, **13**: 1098-1101.

[113] Zhang P, Guo ZP, Huang YD, *et al*. Synthesis of Co_3O_4/carbon composite nanowires and their electrochemical properties. *J Power Sources* 2011, **196**: 6987-6991.

[114] Bonino CA, Ji LW, Lin Z, *et al*. Electrospun carbon-tin oxide composite nanofibers for use as lithium ion battery anodes. *Acs Appl Mater Interf* 2011, **3**: 2534-2542.

[115] Chang DR, Heo GS. Fabrication and electrochemical characterization of carbon nanofibers by electrospinning with various MnO_2 contents. *E-Polymers*, 2011, **075**.

[116] Cheah YL, Gupta N, Pramana SS, *et al*. Morphology, structure and electrochemical properties of single phase electrospun vanadium pentoxide nanofibers for lithium ion batteries. *J Power Sources* 2011, **196**: 6465-6472.

[117] Chen LJ, Liao JD, Chuang YJ, *et al*. Synthesis and characterization of PVP/$LiCoO_2$ nanofibers by electrospinning route. *J Appl Polym Sci* 2011, **121**: 154-160.

[118] Dong ZX, Kennedy SJ, Wu YQ. Electrospinning materials for energy-related applications and devices. *J Power Sources* 2011, **196**: 4886-4904.

[119] Jung HR, Cho SJ, Kim KN, *et al*. Electrochemical properties of electrospun Cu_xO (x =1, 2)-embedded carbon nanofiber with EXAFS analysis. *Electrochim Acta* 2011, **56**: 6722-6731.

[120] Wang L, We Lj, Li ZH, *et al.* Synthesis and electrochemical properties of $Li_2ZnTi_3O_8$ fibers as an anode material for lithium-ion batteries. *Electrochim Acta* 2011, **56**: 5343-5346.

[121] Croce F, Focarete ML, Hassoun J, *et al.* A safe, high-rate and high-energy polymer lithium-ion battery based on gelled membranes prepared by electrospinning. *Energy Environ Sci* 2011, **4**: 921-927.

[122] Dai YQ, Liu WY, Formo E, *et al*. Ceramic nanofibers fabricated by electrospinning and their applications in catalysis, environmental science, and energy technology. *Polym Adv Technol* 2011, **22**: 326-338.

[123] Kong JH, Wong SY, Zhang Y, *et al*. One-dimensional carbon-SnO_2 and SnO_2 nanostructures via single-spinneret electrospinning: Tunable morphology and the underlying mechanism. *J Mater Chem* 2011, **21**: 15928-15934.

[124] Lijo F, Marsano E, Vijila C, *et al.* Electrospun polyimide/titanium dioxide composite nanofibrous membrane by electrospinning and electrospraying. *J Nanosci Nanotechnol* 2011, **11**: 1154-1159.

[125] Mu JB, Chen B, Guo ZC, *et al.* Tin oxide (SnO_2) nanoparticles/electrospun carbon nanofibers (CNFs) heterostructures: controlled fabrication and high capacitive behavior. *J Colloid Interf Sci* 2011, **356**: 706-712.

[126] Hwang DK, Kim S, Lee JH, *et al*. Phase evolution of perovskite $LaNiO_3$ nanofibers for supercapacitor application and p-type gas sensing properties of LaOCl-NiO composite nanofibers. *J Mater Chem* 2011, **21**: 1959-1965.

[127] Yuan T, Zhao BT, Cai R, *et al*. Electrospinning based fabrication and performance improvement of film electrodes for lithium-ion batteries composed of TiO_2 hollow fibers. *J Mater Chem* 2011, **21**: 15041-15048.

[128] Zhang XW, Ji LW, Toprakci O, *et al*. Electrospun nanofiber-based anodes, cathodes, and separators for advanced lithium-ion batteries. *Polym Rev* 2011, **51**: 239-264.

[129] Zhu CB, Yu Y, Gu L, *et al*. Electrospinning of highly electroactive carbon-coated single-crystalline $LiFePO_4$ nanowires. *Angewandte Chemie Inter Ed* 2011, **50**: 6278-6282.

[130] Jung HR, Lee WJ. Preparation and characterization of Ni-Sn/carbon nanofibers composite anode for lithium ion battery. *J Electrochem Soc* 2011, **158**: A644-A652.

[131] Laudenslager MJ, Scheffler RH, Sigmund WM. Electrospun materials for energy harvesting, conversion, and storage: A review. *Pure Appl Chem* 2010, **82**: 2137-2156.

[132] Luo W, Hu XL, Sun YM, *et al*. Electrospinning of

carbon-coated MoO_2 nanofibers with enhanced lithium-storage properties. *Phys Chem Chem Phys* 2011, **13:** 16735-16740.

[133] Mai LQ, Xu L, Han CH, *et al.* Electrospun ultralong hierarchical vanadium oxide nanowires with high performance for lithium ion batteries. *Nano Lett* 2010, **10**: 4750-4755.

[134] Barth S, Hernandez-Ramirez F, Holmes JD, *et al*. Synthesis and applications of one-dimensional semiconductors. *Prog Mater Sci* 2010, **55**: 563-627.

[135] Lee YS, Jeong YB, Kim DW. Cycling performance of lithium-ion batteries assembled with a hybrid composite membrane prepared by an electrospinning method. *J Power Sources* 2010, **195**: 6197-6201.

[136] Li LM, Yin XM, Liu S, *et al.* Electrospun porous SnO_2 nanotubes as high capacity anode materials for lithium ion batteries. *Electrochem Comm* 2010, **12**: 1383-1386.

[137] Miao JJ, Miyauchi M, Simmons TJ, *et al*. Electrospinning of nanomaterials and applications in electronic components and devices. *J Nanosci Nanotechnol* 2010, **10**: 5507-5519.

[138] Yang ZX, Du GD, Guo ZP, *et al.* Easy preparation of SnO_2@carbon composite nanofibers with improved lithium ion storage properties. *J Mater Res* 2010, **25**: 1516-1524.

[139] Liu HQ, Yang JX, Liang JH, *et al*. ZnO nanofiber and nanoparticle synthesized through electrospinning and their photocatalytic activity under visible light. *J Am Ceram Soc* 2008, **91**: 1287-1291.

[140] Neubert S, Pliszka D, Thavasi V, *et al*. Conductive electrospun PANi-PEO/TiO_2 fibrous membrane for photo catalysis. *Mater Sci Eng B* 2011, **176**: 640-646.

[141] Reddy KR, Nakata K, Ochiai T, *et al.* Nanofibrous TiO_2-core/conjugated polymer-sheath composites: synthesis, structural properties and photocatalytic activity. *J Nanosci Nanotechnol* 2010, **10**: 7951-7957.

[142] Yi C, Nirmala R, Navamathavan R, *et al*. Preparation of photocrosslinkable polystyrene methylene cinnamate nanofibers via electrospinning. *J Nanosci Nanotechnol* 2011, **11**: 8474-8480.

[143] Huang JS, Wang DW, Hou HQ, *et al*. Electrospun palladium nanoparticle-loaded carbon nanofibers and their electrocatalytic activities towards hydrogen peroxide and NADH. *Adv Funct Mater* 2008, **18**: 441-448.

[144] Ostermann R, Li D, Yin YD, *et al*. V_2O_5 nanorods on TiO_2 nanofibers: a new class of hierarchical nanostructures enabled by electrospinning and calcination. *Nano Lett* 2006, **6**: 1297-1302.

[145] Cao TP, Li YJ, Wang CH, *et al*. A facile in situ hydrothermal method to $SrTiO_3$/TiO_2 nanofiber heterostructures with high photocatalytic activity. *Langmuir* 2011, **27**: 2946-2952.

[146] Li CJ, Wang JN, Li XY, *et al*. Functionalization of electrospun magnetically separable TiO_2-coated $SrFe_{12}O_{19}$ nanofibers: strongly effective photocatalyst and magnetic separation. *J Mater Sci* 2011, **46**: 2058-2063.

[147] Li XY, Wang, FF, Qian QR, *et al*. Ag/TiO_2 nanofibers heterostructure with enhanced photocatalytic activity for parathion. *Mater Lett* 2012, **66**: 370-373.

[148] Ochanda FO, Barnett MR. Synthesis and characterization of silver nanoparticles and titanium oxide nanofibers: toward multifibrous nanocomposites. *J Am Ceram Soc* 2010, **93**: 2637-2643.

[149] Su CY, Shao CL, Liu YC. Electrospun nanofibers of TiO_2/CdS heteroarchitectures with enhanced photocatalytic activity by visible light. *J Colloid Interf Sci* 2011, **359**: 220-227.

[150] Wang CH, Zhang XT, Shao CL, *et al*. Rutile TiO_2 nanowires on anatase TiO_2 nanofibers: A branched heterostructured photocatalysts via interface-assisted fabrication approach. *J Colloid Interf Sci* 2011, **363**: 157-164.

[151] Zhang P, Shao CL, Zhang ZY, *et al*. Core/shell nanofibers of TiO_2@carbon embedded by Ag nanoparticles with enhanced visible photocatalytic activity. *J Mater Chem* 2011, **21**: 17746-17753.

[152] Zhang ZY, Shao CL, Li XT, *et al.* Electrospun nanofibers of p-type NiO/n-type ZnO heterojunctions with enhanced photocatalytic activity. *Acs Appl Mater Interf* 2011, **2**: 2915-2923.

[153] Choi SK, Kim S, Lim SK, *et al*. Highly enhanced photocatalytic activities of electrospun mesoporous TiO_2 nanofiber. *Abst Papers Am Chem Soc* 2010, **239**.

[154] Lee JA, Nam YS, Rutledge GC, *et al*. Enhanced photocatalytic activity using layer-by-layer electrospun constructs for water remediation. *Adv Funct*

Mater 2010, **20**: 2424-2429.

[155] Zhang TZ, Ge LQ, Wang X, *et al*. Hollow TiO_2 containing multilayer nanofibers with enhanced photocatalytic activity. *Polymer* 2008, **49**: 2898-2902.

[156] Ke XB, Ribbens S, Fan YQ, *et al*. Integrating efficient filtration and visible-light photocatalysis by loading Ag-doped zeolite Y particles on filtration membrane of alumina nanofibers. *J Membrane Sci* 2011, **375**: 69-74.

[157] Ke XB, Zheng ZF, Liu HW, *et al.* High-flux ceramic membranes with a nanomesh of metal oxide nanofibers. *J Phys Chem B* 2008, **112**: 5000-5006.

[158] Zhao YF, Sugiyama S, Miller T, *et al*. Nanoceramics for blood-borne virus removal. *Expert Rev Medical Devices* 2008, **5**: 395-405.

[159] Cao YH, Wu H, Hu LB, *et al*. Electrospun SiO_{2n} nanofiber as a battery separator. *Abst Papers Am Chem Soc* 2011, **241**.